

## Supporting Information for

### Naphthoxaphospholes as examples of fluorescent *phospha-acenes*

Feng Li Laughlin,<sup>a</sup> Arnold L. Rheingold,<sup>b</sup> Nihal Deligonul,<sup>a</sup> Brynna Laughlin,<sup>c</sup> Lee J. Higham,<sup>d</sup> and John D. Protasiewicz<sup>\*a</sup>

#### Syntheses and NMR Properties

Compounds **1** and **2** were prepared using slight modifications of reported procedures (Dhawan, B.; Redmore, D. *J. Org. Chem.* **1984**, *49*, 4018, Dhawan, B.; Redmore, D. *J. Org. Chem.* **1991**, *56*, 833.).

#### Diethyl(2-naphthyl)phosphate (**1**):

Triethylamine (17.5 mL, 89.7 mmol) was added drop wise to a mixture containing 2-naphthol (10.0 g, 69.4 mmol) and diethyl chlorophosphate (12.1 mL, 83.2 mmol) in THF 150 mL in a 500 mL round bottom flask with a stir bar. The solution was stirred for 12 hours. Aqueous HCl solution (1.2 M, 100 mL) was added, the mixture solution was stirred until precipitate disappeared, and diethyl ether 100 mL was added to extract the product. The organic layer was separated and washed successively with degassed solution of aqueous HCl (1.2 M, 100mL), aqueous NaOH (1 M, 100mL), distilled water and was dried over anhydrous sodium sulfate. The solvent was removed by rotary evaporation to yield brown liquid **1** (18.7 g, 95.9%); <sup>1</sup>H NMR (CDCl<sub>3</sub>): δ 7.79 (m, 3H) 7.69 (s, 1H), 7.43 (m, 2H), 7.36 (m, 1H), 4.23 (m, 4H), 1.34 (m, 6H); <sup>31</sup>P{<sup>1</sup>H} NMR (CDCl<sub>3</sub>): δ -6.1 (s); <sup>13</sup>C{<sup>1</sup>H} NMR (CDCl<sub>3</sub>): δ 148.3 (d, *J*<sub>PC</sub> = 6.9 Hz), 133.8, 130.8, 129.8, 127.6, 127.5, 126.6, 125.4, 120.0 (d, *J*<sub>PC</sub> = 5.3 Hz), 116.3 (d, *J*<sub>PC</sub> = 4.8 Hz), 64.6 (d, *J*<sub>PC</sub> = 6.0 Hz), 16.1 (d, *J*<sub>PC</sub> = 6.6 Hz).

### Diethyl(3-hydroxy-2-naphthyl)phosphonate ( **2** ):

To a solution of diisopropylamine (15.1 mL, 107 mmol) in 50 mL THF, at -78 °C in a nitrogen atmosphere in a 500 mL round bottom flask with a stir bar, nBuLi (2.5 M in hexane, 42.8 mL, 107 mmol) was added. The mixture was stirred for 30 minutes to allow white slurry lithium diisopropylamide (LDA) formed. Diethyl (2-naphthyl) phosphate (**1**, 15.0 g, 53.5 mmol) was dissolved in 25 mL THF in a 50 mL round bottom flask, and then transferred to LDA by cannula. The mixture solution was stirred for 2 h at -78 °C, brought to room temperature and then poured over saturated ammonium chloride aqueous solution (250 mL). The solution was stirred for 15 min. until precipitate was dissolved, and the product was extract with CH<sub>2</sub>Cl<sub>2</sub> 300 mL. Organic layer was separated and washed by distilled water twice, dried over anhydrous sodium sulfate. The solvent was removed by rotary evaporation to yield brown liquid, which solidified upon cooling. Clear crystals **2** were obtained by dissolving warm hexanes and cooling to -4 °C (5.24 g, 51.4%) <sup>1</sup>H NMR (CDCl<sub>3</sub>): δ 9.99 (s, 1H, OH) 8.02 (d, 1H, <sup>3</sup>J<sub>PH</sub> = 16.4 Hz), 7.79 (m, 1H), 7.70 (m, 1H), 7.49 (m, 1H), 7.33 (m, 2H), 4.16 (m, 4H), 1.35 (m, 6H); <sup>31</sup>P{<sup>1</sup>H} NMR (CDCl<sub>3</sub>): δ 21.9 (s); <sup>13</sup>C{<sup>1</sup>H} NMR (CDCl<sub>3</sub>): δ 156.7 (d, J<sub>PC</sub> = 7.6 Hz), 137.7 (d, J<sub>PC</sub> = 2.0 Hz), 134.1 (d, J<sub>PC</sub> = 5.7 Hz), 128.7, 128.6, 127.3 (d, J<sub>PC</sub> = 15.3 Hz), 126.5, 123.9, 112.4 (d, J<sub>PC</sub> = 179.6 Hz), 111.6 (d, J<sub>PC</sub> = 11.5 Hz), 62.9 (d, J<sub>PC</sub> = 4.7 Hz), 16.2 (d, J<sub>PC</sub> = 6.6 Hz); mp: 110-113 °C; Elemental Analysis: Calc. for C<sub>15</sub>H<sub>15</sub>OP (M.W. 280.26), C 60.00%, H 6.11%; found: C 60.32%, H 6.17%.

## Crystallography

Crystal data and collection parameters for crystal structure of **2**, **4b** and **4d** are provided in Table S1. Compound **2** was analyzed at Chemistry Department, Case Western Reserve University, while compounds **4b** and **4d** were examined at Department of Chemistry and Biochemistry, University of California, San Diego. Single-crystal diffraction studies at CWRU were performed using a Bruker AXS SMART APEX II CCD diffractometer using monochromatic Mo K $\alpha$  radiation with the omega scan technique. The unit cell was determined using SMART<sup>a</sup> and SAINT<sup>b</sup>. Data collection for compound **2** was conducted at 100 K (-173.5 °C). The structure was solved by direct method and refined by full matrix least squares against  $F^2$  with all reflections using SHELXTL.<sup>c</sup> Refinement of extinction coefficients was found to be insignificant. All non-hydrogen atoms were refined anisotropically. All hydrogen atoms were placed in standard calculated positions and all hydrogen atoms were refined with an isotropic displacement parameter 1.2 times that of the adjacent carbon. Further details for all structures are accessible in the accompanying cif files for each structure. CCDC 878276-878278 contains the supplementary crystallographic data for this paper. These data can be obtained free of charge from The Cambridge Crystallographic Data Centre via [www.ccdc.cam.ac.uk/data\\_request/cif](http://www.ccdc.cam.ac.uk/data_request/cif).

Compound **2**. X-ray quality crystals were grown at low temperature (- 45°C) in hexanes.

Compound **4b**. X-ray quality crystals were dissolved in hot diethyl ether and grown at room temperature in dry box.

Compound **4d**. X-ray quality crystals were dissolved in hot CH<sub>2</sub>Cl<sub>2</sub> and grown at room temperature in dry box.

<sup>a</sup> Bruker Advanced X-ray Solutions. SMART for WNT/2000 (Version 5.628); Bruker AXS Inc.: Madison, WI, 1997–2002

<sup>b</sup> Bruker Advanced X-ray Solutions. SAINT (Version 6.45); Bruker AXS Inc.: Madison, WI, 1997–2003

<sup>c</sup> Bruker Advanced X-ray Solutions. SHELXTL (Version 6.10); Bruker AXS Inc.: Madison, WI, 2000.

	<b>2</b>	<b>4b</b>	<b>4d</b>
formula	C14 H12 O4 P	C21 H21 O P	C18 H13 O P
fw	275.21	320.35	276.25
space group	P2(1)/c	P2(1)2(1)2(1)	P2(1)
temperature (K)	170	100	100
<i>a</i> (Å)	9.6672(1)	6.5436(1)	11.755(1)
<i>b</i> (Å)	11.5278(2)	13.3825(1)	7.3511(2)
<i>c</i> (Å)	12.8735(2)	18.4075(2)	16.433(1)
<i>α</i> (deg)	90.00	90.00	90.00
<i>β</i> (deg)	102.6630(10)	90.00	108.790(3)
<i>γ</i> (deg)	90.00	90.00	90.00
<i>V</i> (Å <sup>3</sup> )	1399.7(2)	1611.94(2)	1344.3(4)
<i>Z</i>	4	4	4
density <sub>calc</sub> (g/cm <sup>3</sup> )	1.306	1.320	1.365
radiation	MoK $\alpha$ ( $\lambda = 0.71073$ Å)	MoK $\alpha$ ( $\lambda = 0.71073$ Å)	MoK $\alpha$ ( $\lambda = 0.71073$ Å)
monochromator	graphite	graphite	graphite
detector	CCD area detector	CCD area detector	CCD area detector
no. of reflns measd	hemisphere	hemisphere	hemisphere
2 $\theta$ range (deg)	4.8-55.9	6.60-50.74	5.24-61.4
cryst dimens (mm)	0.42 x 0.29 x 0.10	0.26 x 0.25 x 0.20	0.29 x 0.24 x 0.08
no. of reflns measd	16803	4287	10573
no. of unique reflns	3362	2336	6734
no. of observations	3362	2336	6734
no. of params	177	209	363
<i>R</i> , <i>R<sub>w</sub></i> , <i>R<sub>all</sub></i>	0.0513, 0.1702, 0.0551	0.0425, 0.1110, 0.0462	0.0528, 0.1239, 0.0772
GOF	1.132	1.070	1.012

**Table S1.** Crystal data and collection parameters of compounds **2**, **4b** and **4d**

## Absorption and Emission Spectroscopy of NOPs

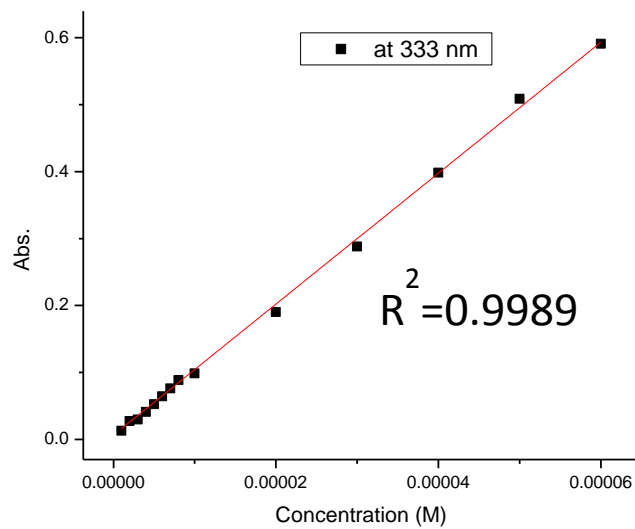
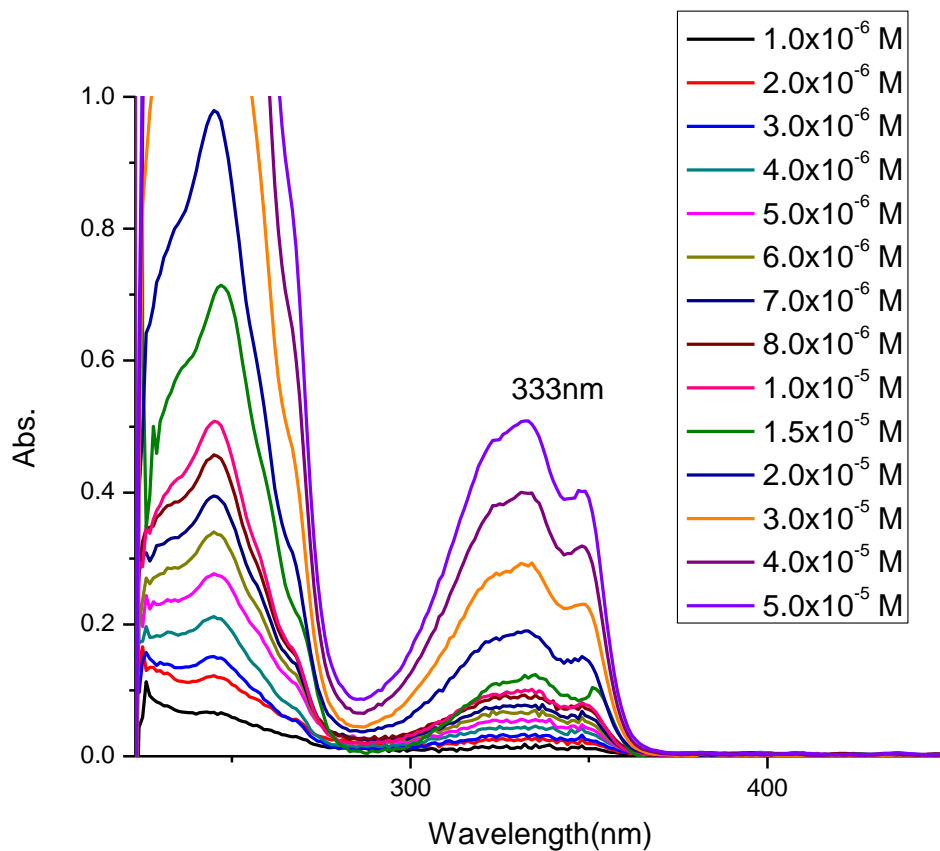


**Figure S2.** UV-vis absorption spectrum of <sup>t</sup>Bu-NOP (**4a**) and Beer's Law plot.

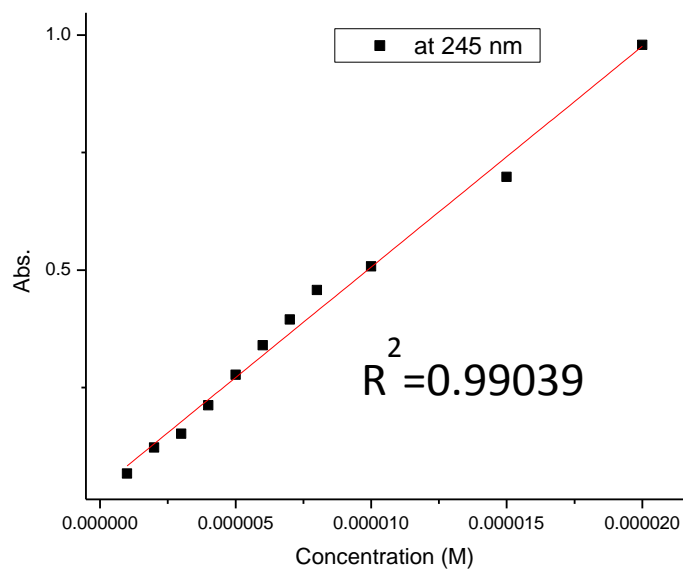
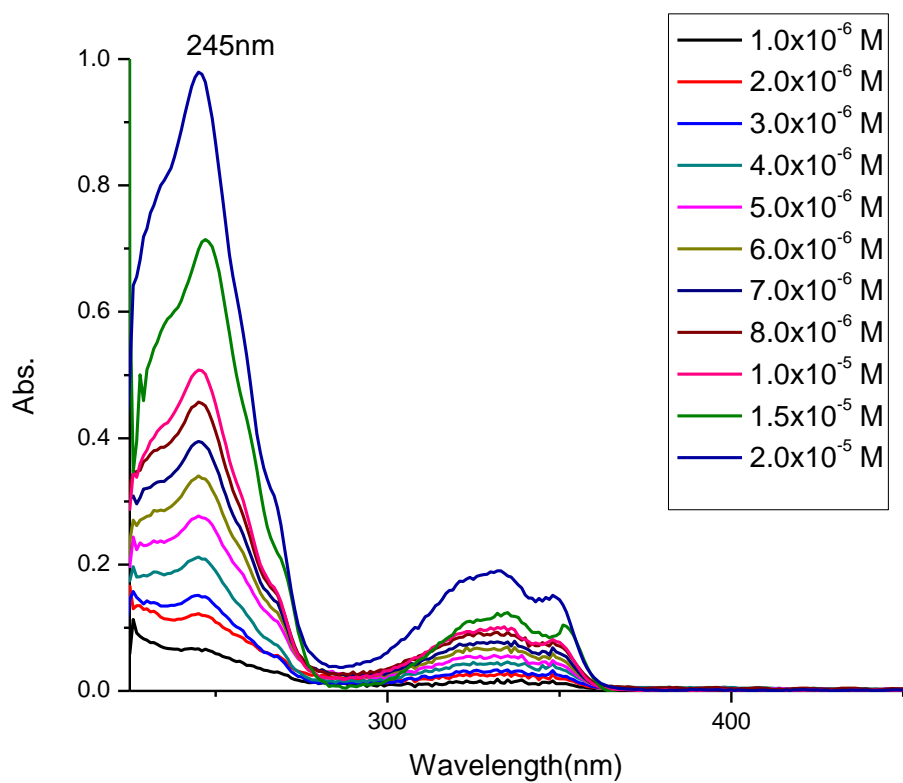


**Figure S3.** UV-vis absorption spectrum of *t*Bu-NOP (**4a**) and Beer's Law plot

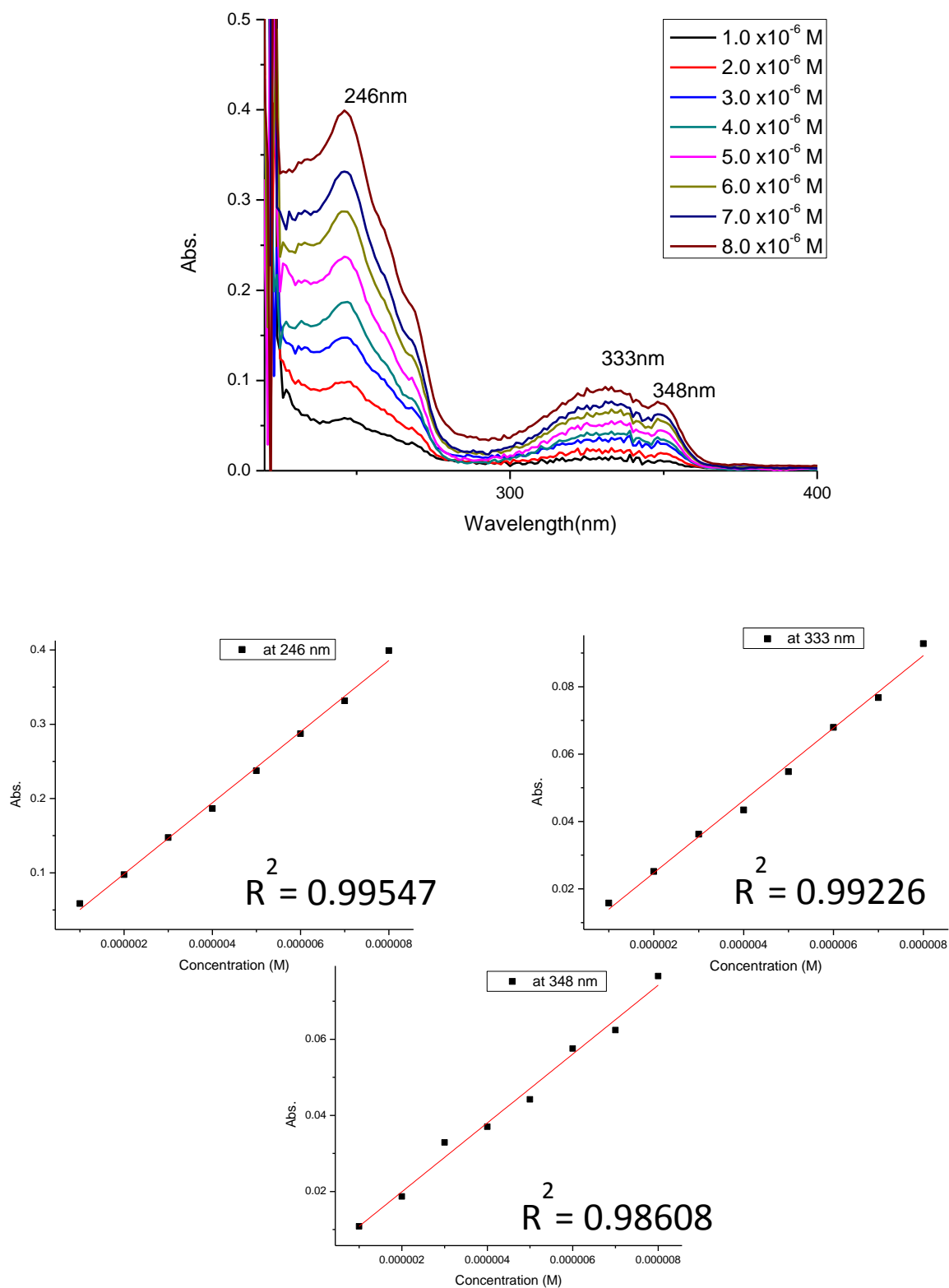


**Figure S4.** UV-vis absorption spectrum of Ad-NOP (**4b**) and Beer's Law plots

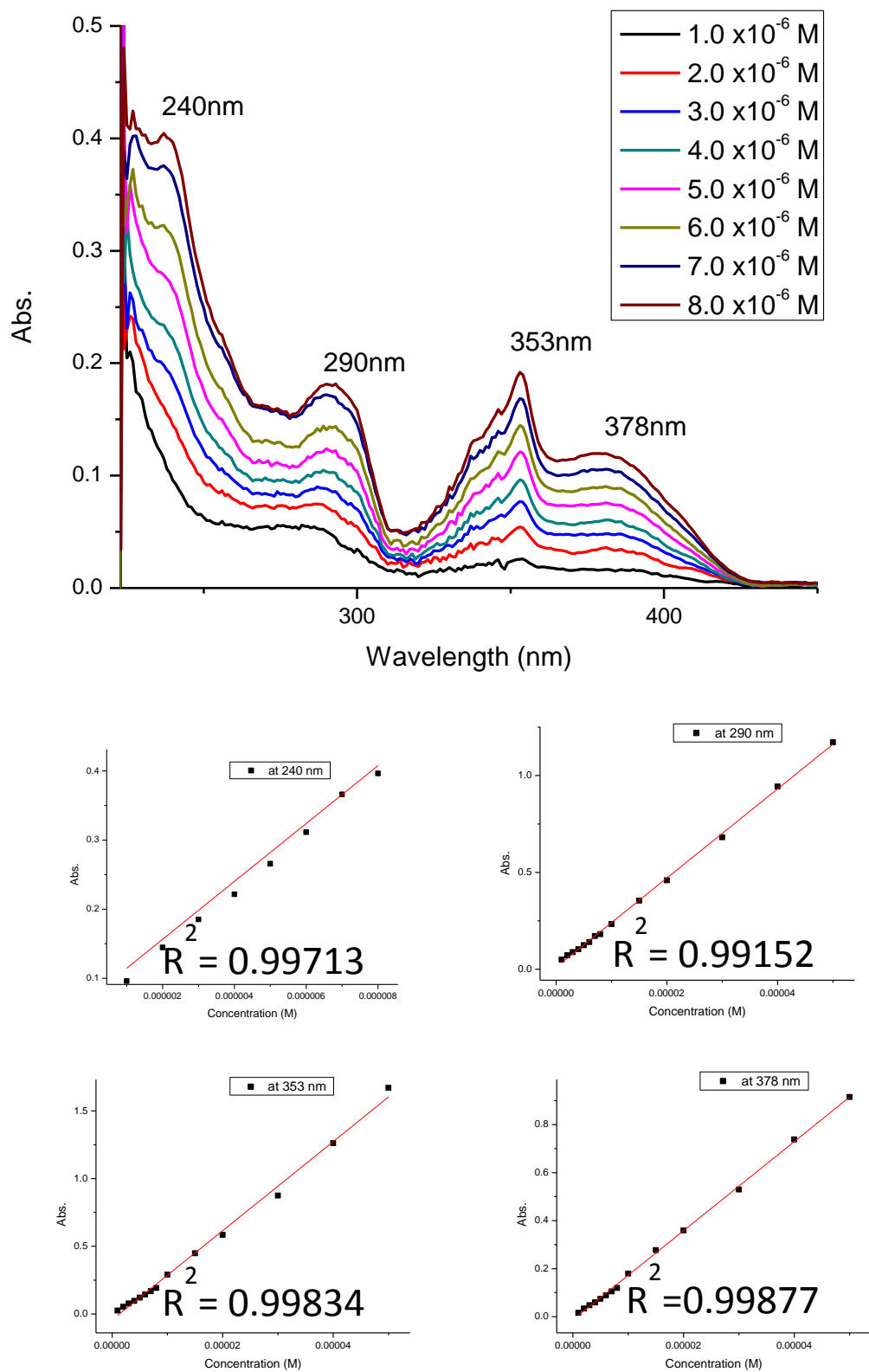


**Figure S5.** UV-vis absorption spectrum of  $C_6H_5-NOP$  (**4c**) and Beer's Law plots

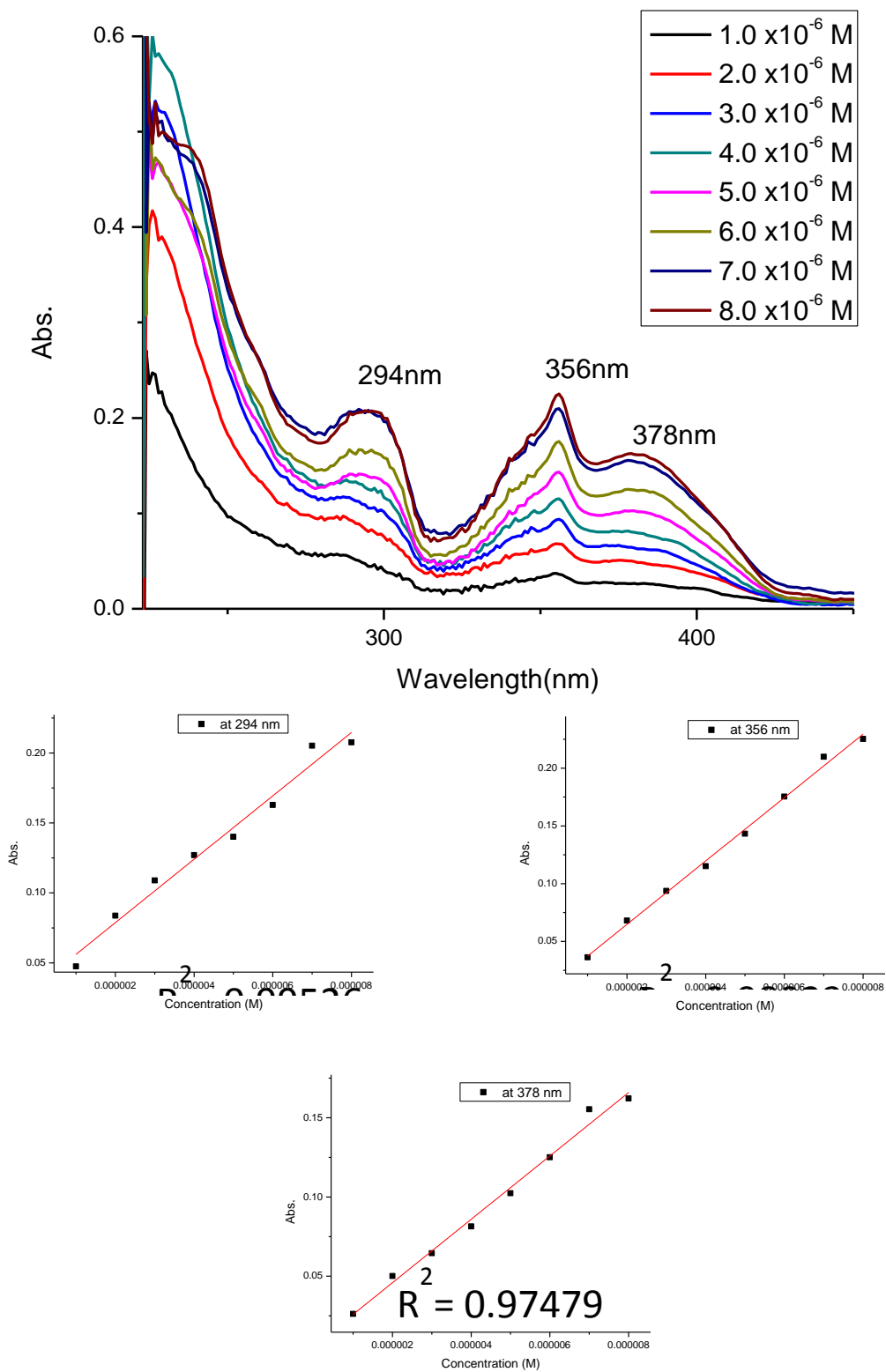


**Figure S6.** UV-vis absorption spectrum of 4-MeC<sub>6</sub>H<sub>4</sub>-NOP (**4d**) and Beer's Law plots

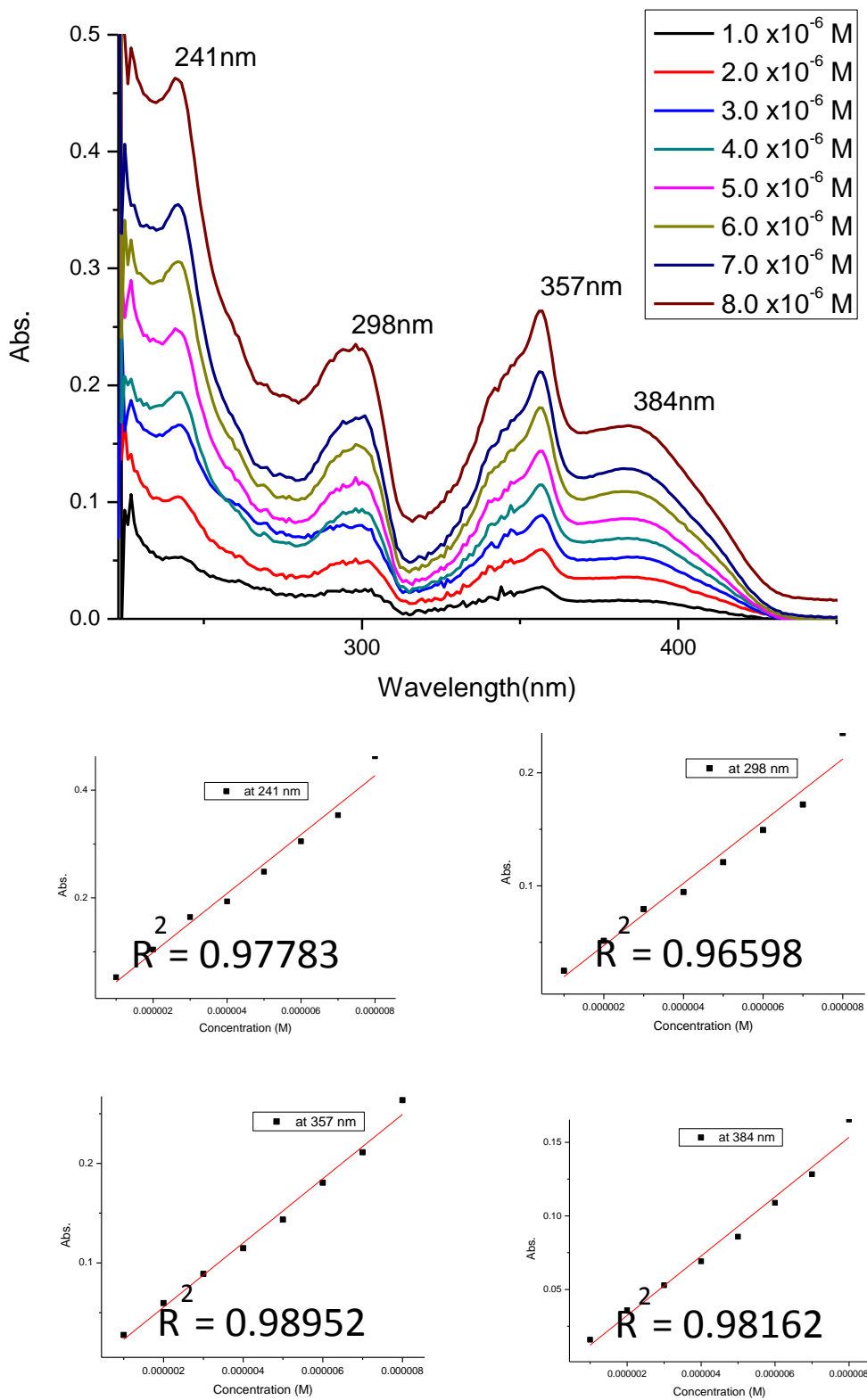


**Figure S7.** UV-vis absorption spectrum of 4-ClC<sub>6</sub>H<sub>4</sub>-NOP (**4e**) and Beer's Law plots

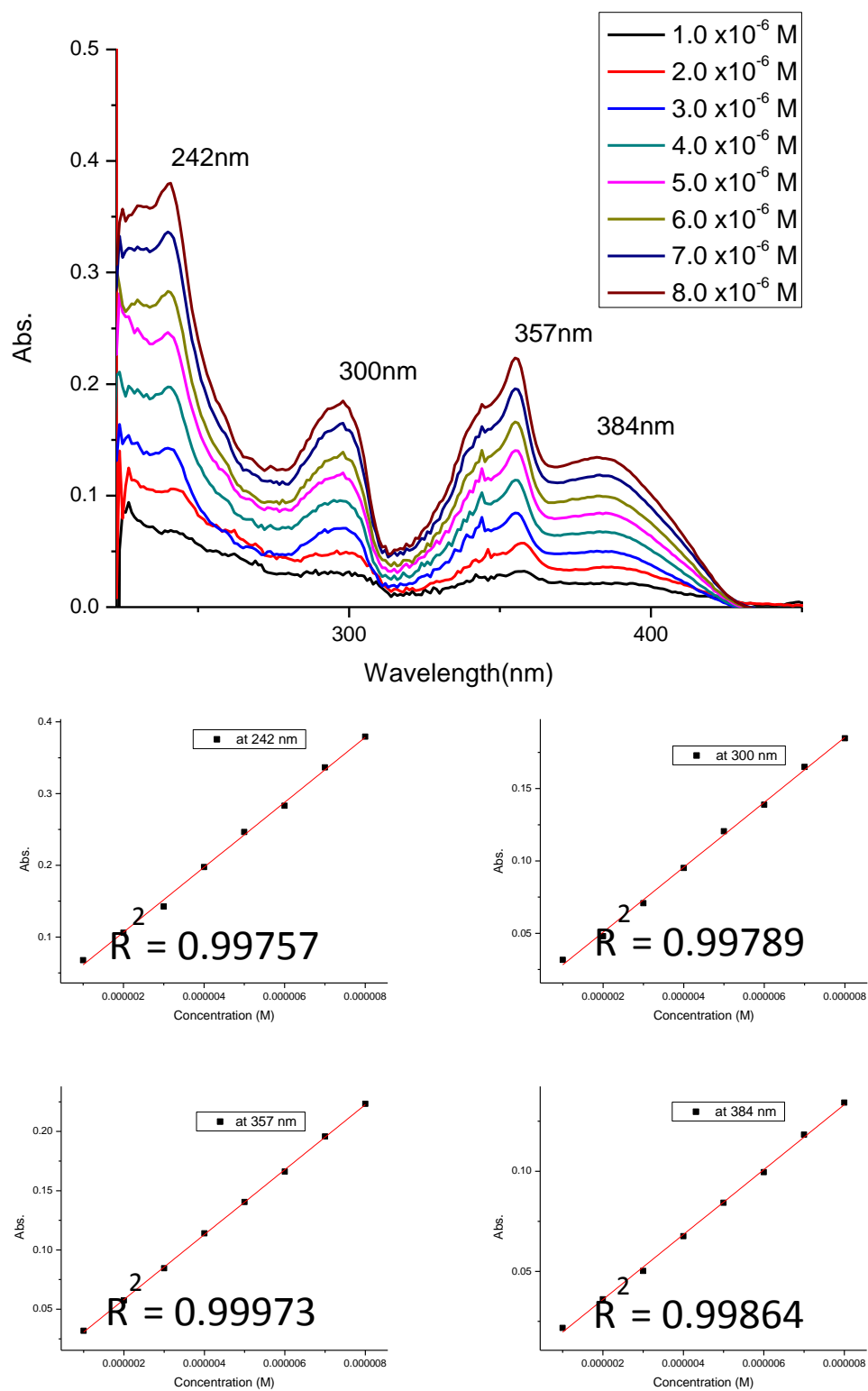


**Figure S8.** UV-vis absorption spectrum of 4-BrC<sub>6</sub>H<sub>4</sub>-NOP (**4f**) and Beer's Law plots

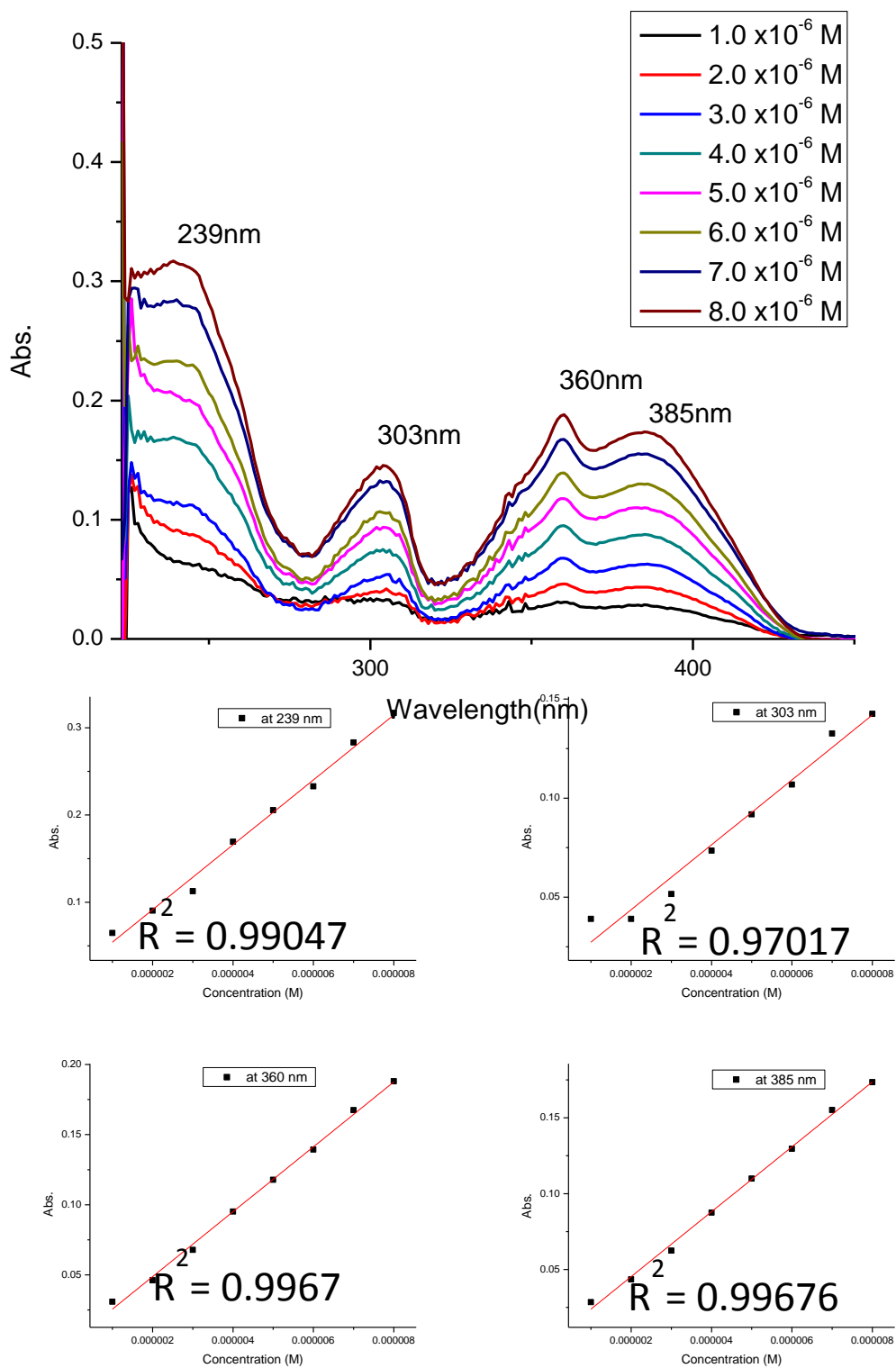


**Figure S9.** UV-vis absorption spectrum of 4-MeOC<sub>6</sub>H<sub>4</sub>-NOP (4g) and Beer's Law plots

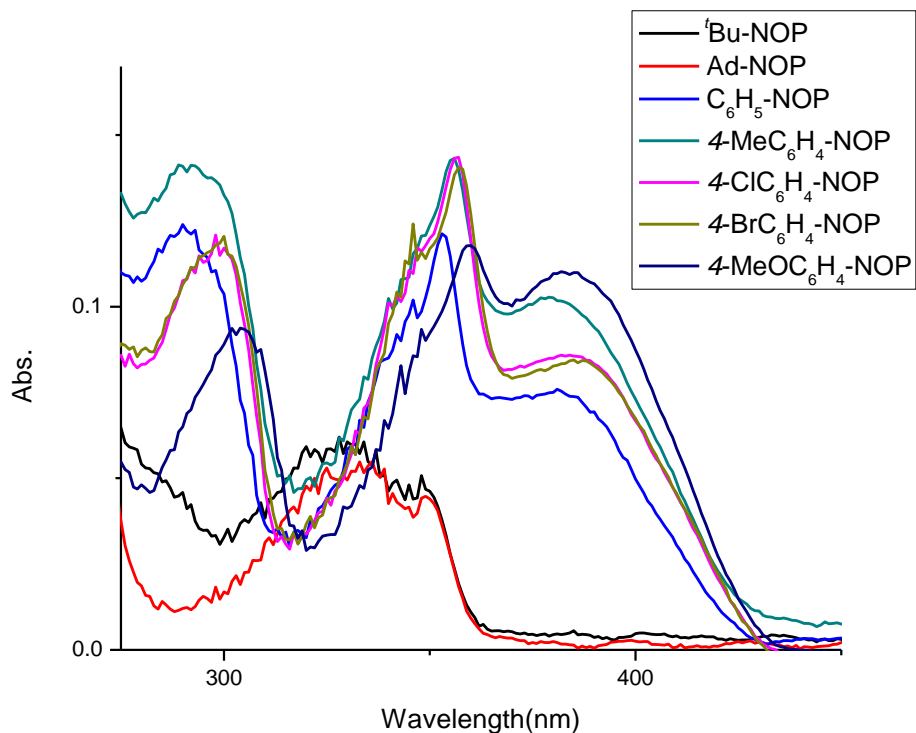


**Figure S10.** UV-vis absorption spectrum of NOPs (**4a-g**) (conc.  $5.0 \times 10^{-6}$  M in  $\text{CH}_2\text{Cl}_2$ )

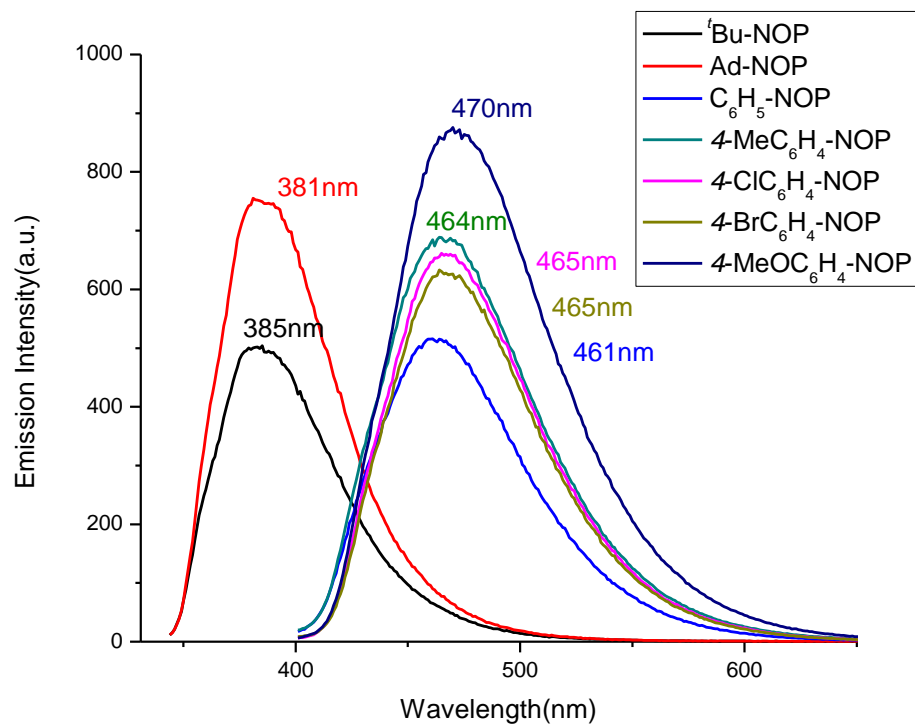


**Figure S11.** Fluorescence emission spectrum of NOPs (**4a-g**) (conc.  $5.0 \times 10^{-6}$  M in  $\text{CH}_2\text{Cl}_2$ )

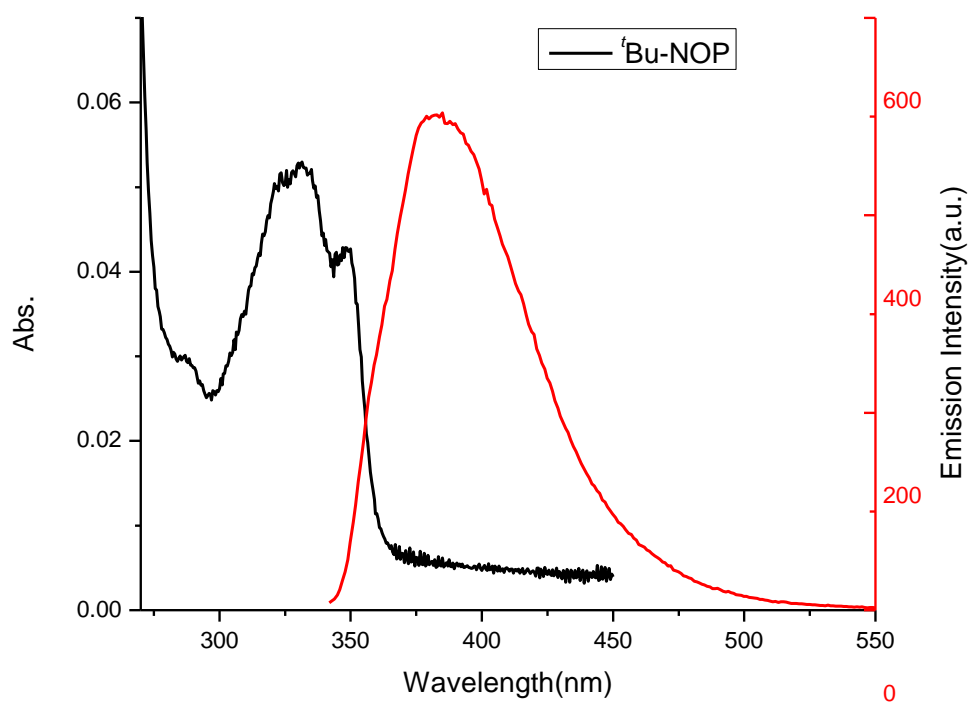


**Figure S12.** UV-vis and Fluorescence of *t*Bu-NOP (**4a**) (conc.  $5.0 \times 10^{-6}$  M in  $\text{CH}_2\text{Cl}_2$ )

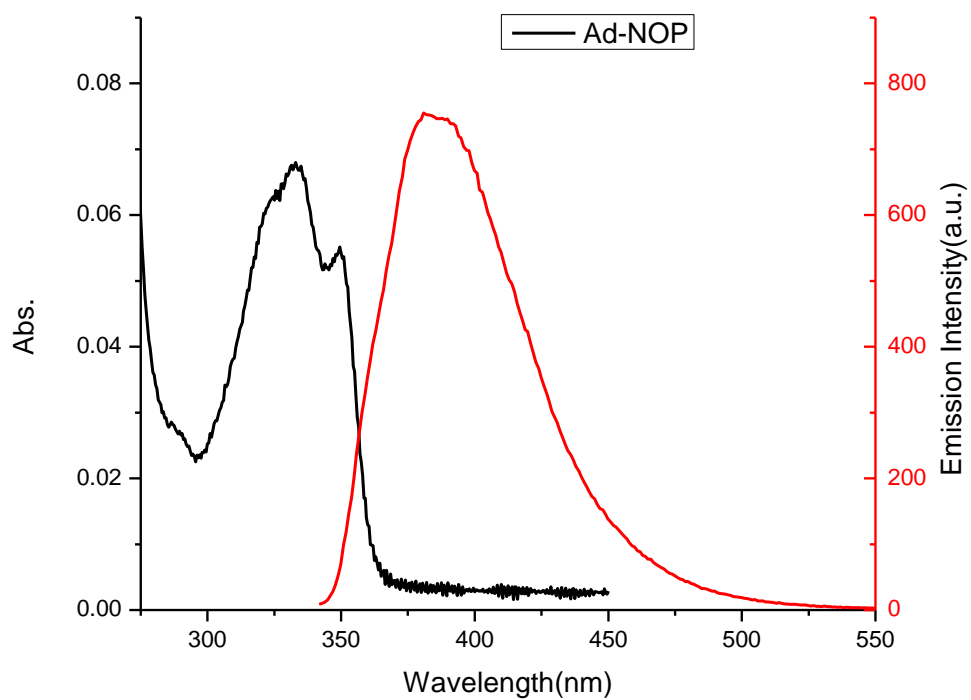


**Figure S13.** UV-vis and Fluorescence of Ad-NOP (**4b**) (conc.  $5.0 \times 10^{-6}$  M in  $\text{CH}_2\text{Cl}_2$ )

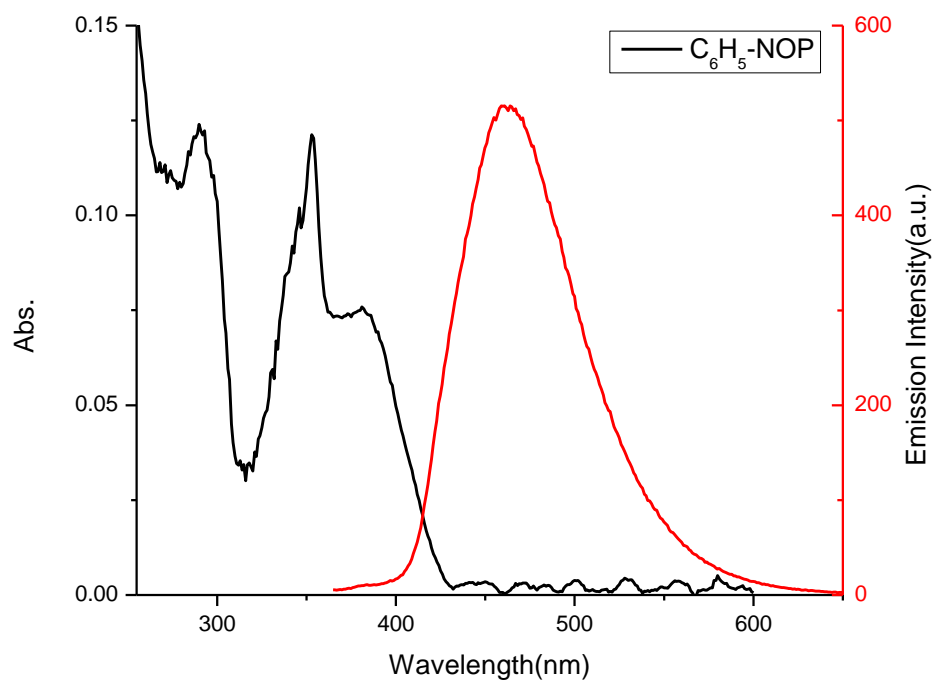


**Figure S14.** UV-vis and Fluorescence of  $C_6H_5-NOP$  (**4c**) (conc.  $5.0 \times 10^{-6}$  M in  $CH_2Cl_2$ )

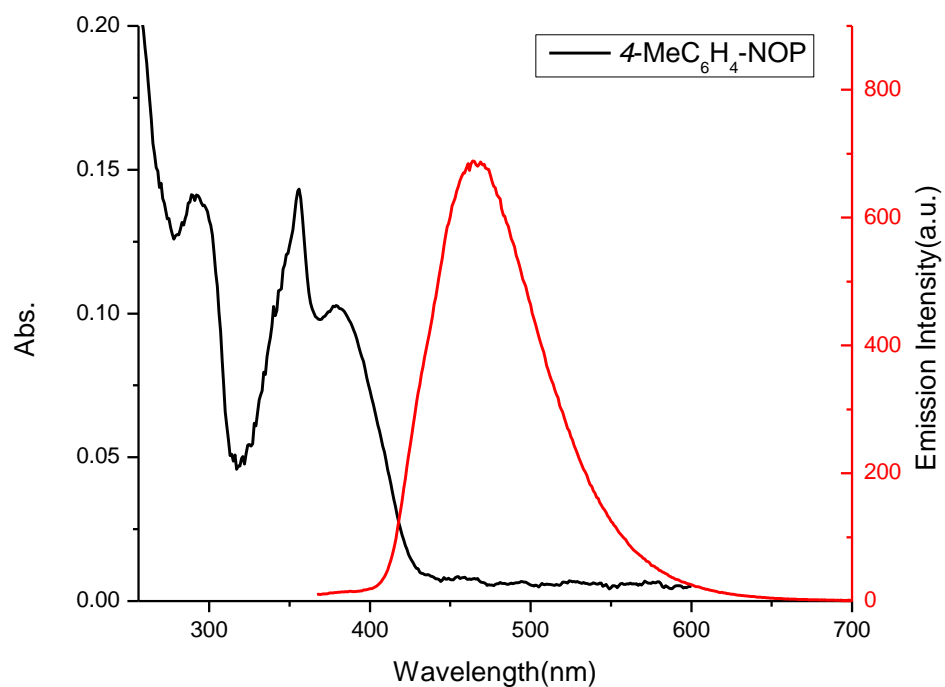


**Figure S15.** UV-vis and Fluorescence of  $4-MeC_6H_4-NOP$  (**4d**) (conc.  $5.0 \times 10^{-6}$  M in  $CH_2Cl_2$ )

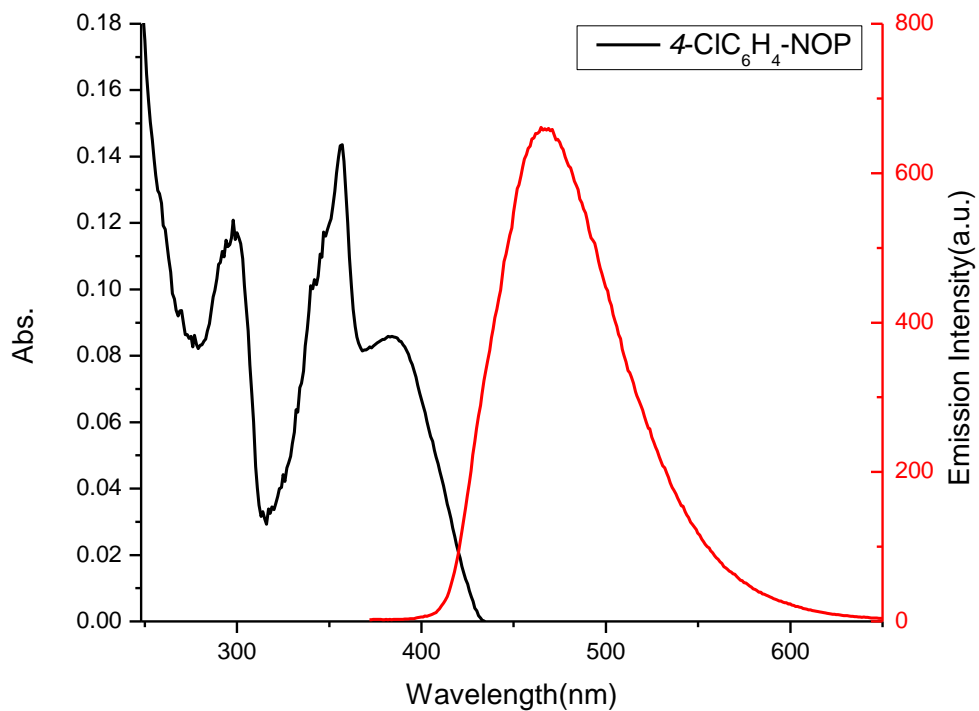


**Figure S16.** UV-vis and Fluorescence of 4-ClC<sub>6</sub>H<sub>4</sub>-NOP (**4e**) (conc.  $5.0 \times 10^{-6}$  M in CH<sub>2</sub>Cl<sub>2</sub>)

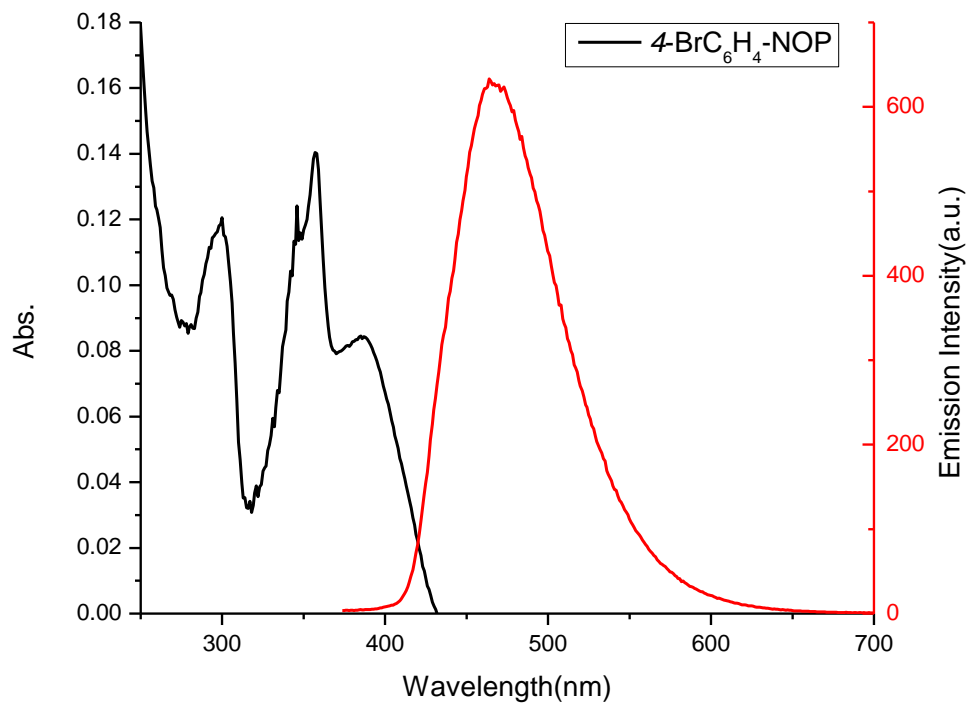


**Figure S17.** UV-vis and Fluorescence of 4-BrC<sub>6</sub>H<sub>4</sub>-NOP (**4f**) (conc.  $5.0 \times 10^{-6}$  M in CH<sub>2</sub>Cl<sub>2</sub>)

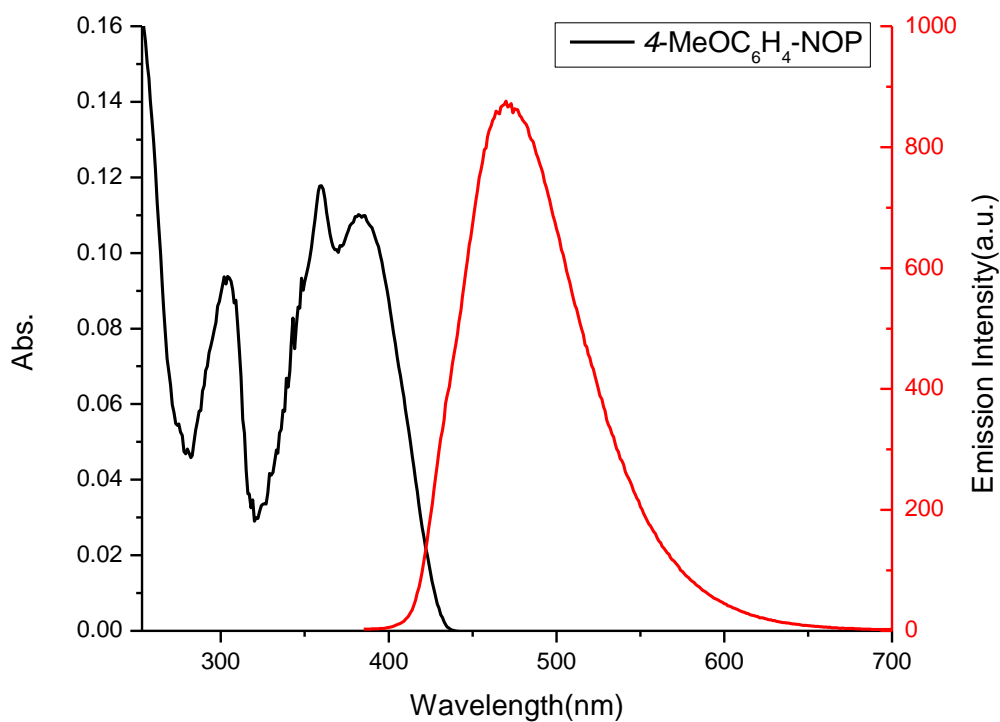


**Figure S18.** UV-vis and Fluorescence of 4-MeOC<sub>6</sub>H<sub>4</sub>-NOP (**4g**) (conc. 5.0 × 10<sup>-6</sup> M in CH<sub>2</sub>Cl<sub>2</sub>)

Compounds	Substitution (R)	$\lambda_{\text{max}}$ (nm)	$\lambda_{\text{F,max}}$ (nm)	$\Phi$	$\tau$ (ns)
<b>4a</b>	<sup>t</sup> Bu	333	385	0.23	1.24(2)
<b>4b</b>	Ad	333	381	0.26	1.26(1)
<b>4c</b>	C <sub>6</sub> H <sub>5</sub>	353	461	0.12	0.76(1)
<b>4d</b>	4-MeC <sub>6</sub> H <sub>4</sub>	356	464	0.14	0.75(1)
<b>4e</b>	4-ClC <sub>6</sub> H <sub>4</sub>	357	465	0.13	0.44(1)
<b>4f</b>	4-BrC <sub>6</sub> H <sub>4</sub>	357	464	0.13	0.80(5)
<b>4g</b>	4-MeOC <sub>6</sub> H <sub>4</sub>	360	470	0.22	0.84(1)

**Table S2.** UV-vis and Fluorescence of NOPs (**4a-g**) (conc. 5.0 × 10<sup>-6</sup> M in CH<sub>2</sub>Cl<sub>2</sub>)

## Electrochemical Studies of NOPs

Cyclic voltammetry experiments were performed in a nitrogen- filled MBraun drybox outfitted with a CH Instrument workstation (CHI630C) at room temperature. Tetrabutylammonium tetrafluoroborate, [<sup>n</sup>Bu<sub>4</sub>N][BF<sub>4</sub>], was recrystallized five times using ethyl acetate and ether, dried thoroughly under vacuum, and stored in the drybox. Ferrocene was purified by sublimation under vacuum and stored in the drybox. All glassware was oven-dried overnight before use. A glassy carbon working electrode was polished with 0.05 μm alumina and thoroughly cleaned and dried before use. A silver wire was utilized as a quasi-reference electrode, and a platinum wire was the counter electrode. All scans were performed at a scan rate of 0.1 V/s unless otherwise stated. All spectra were referenced to SCE using ferrocene as an internal standard.

Solutions with a concentration of 0.001M NOPs in THF were used for reduction analyses. A three-electrode system, with glassy carbon as the working electrode, silver wire as the quasi-reference electrode, and platinum wire as the counter electrode, was utilized. All scans were performed with 0.1 M tetrabutylammonium tetrafluoroborate, [<sup>n</sup>Bu<sub>4</sub>N] [BF<sub>4</sub>], in THF as the supporting electrolyte, with a scan rate of 0.1 V/s. Ferrocene was utilized as an internal reference because of the use of a quasi-reference electrode during analyses. Ferrocene (final concentration 0.001 M) was added after the initial scans of compounds. The reduction potentials were thus referenced to the ferrocene/ferrocenium redox couple versus saturated calomel electrode ( $E_{1/2} = 0.55$  V vs SCE). Reversibility was ascertained by scanning compounds **4c** at various scan rates (25-200 mV) and generating linear plots of scan rates versus  $\Delta E_p$  for both ferrocene and compound **4c** (see Supporting Information), confirming adherence to the Nernst equation.

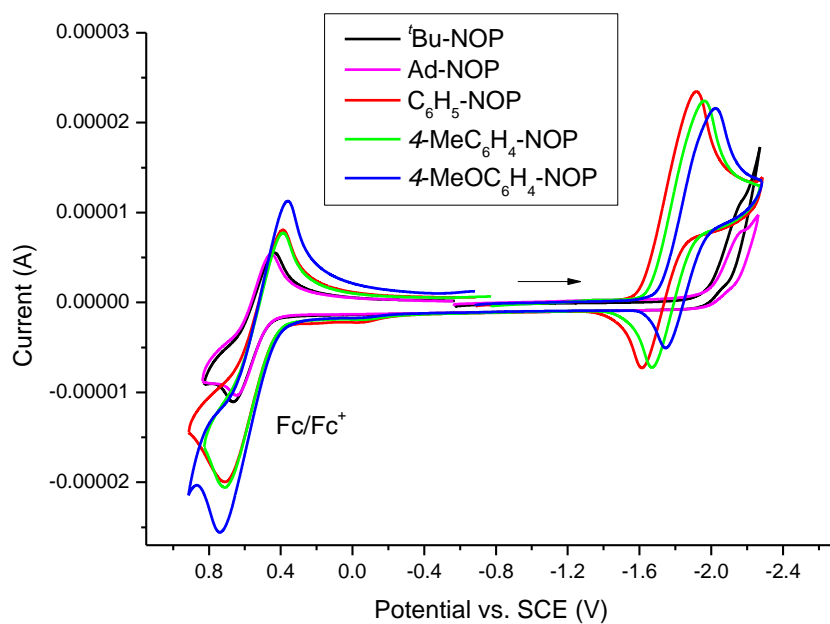


**Figure S19.** Cyclic voltammogram of **4a-d** and **4g** (conc. is 0.001M in THF)

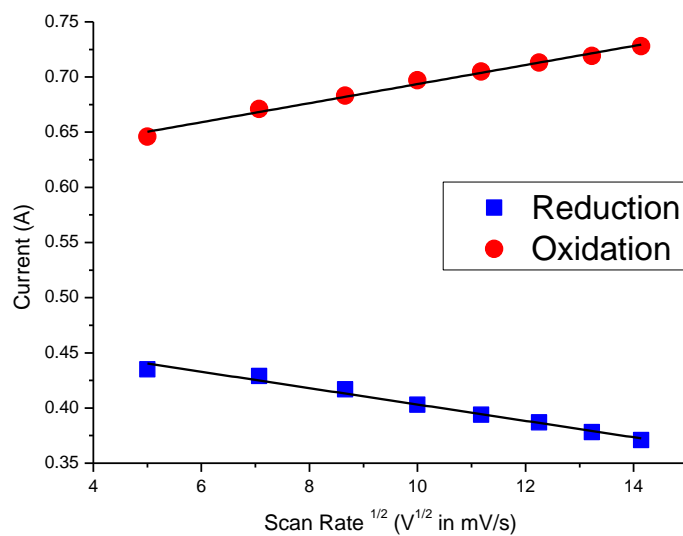


**Figure S20.** Scan rate vs.  $\Delta E_p$  plot of ferrocene redox couple

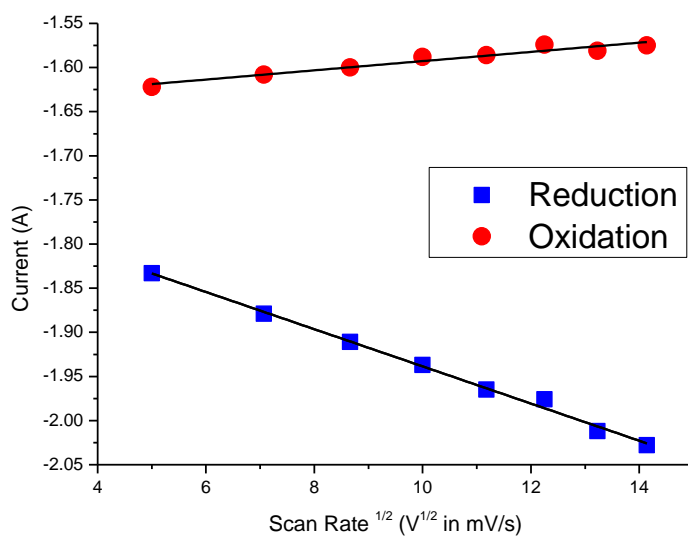


**Figure S21.** Scan rate vs  $\Delta E_p$  plot of the redox couple of compound **4c**

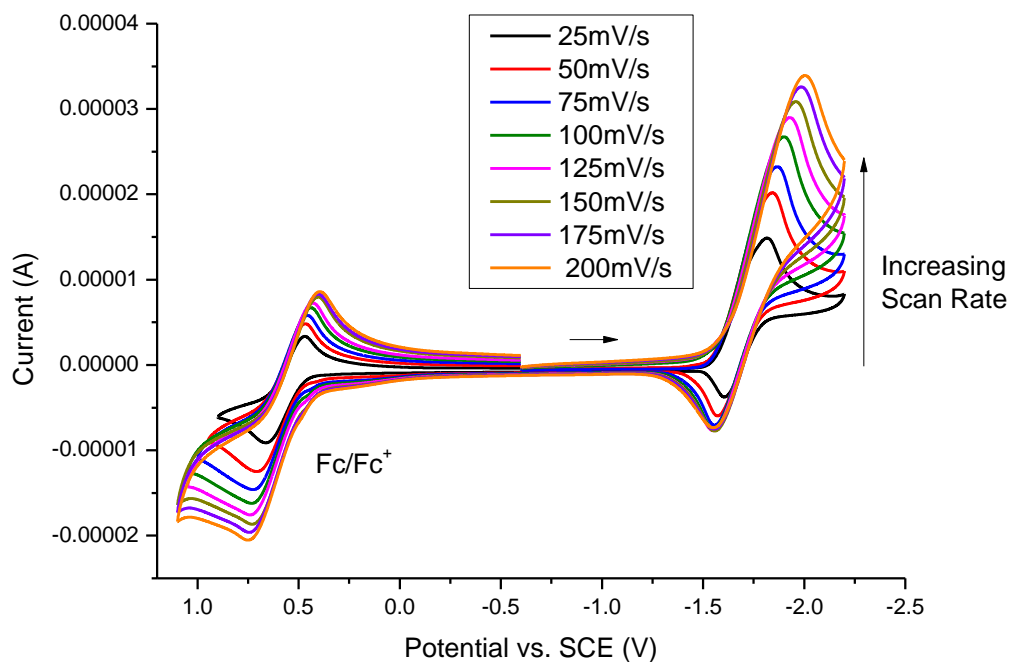
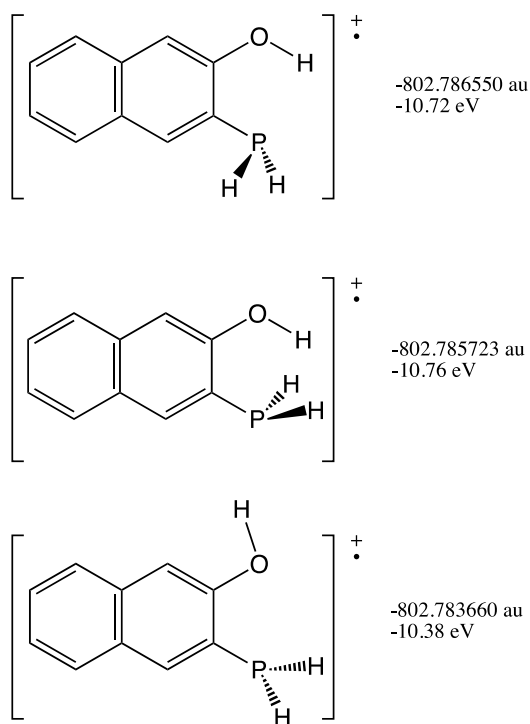


**Figure S22.** Variable scan rate voltammogram for compound **4c** (scan rates of 25 to 200mV/s, conc. is 0.001M in THF)

## Computational Studies of NOPs

Calculations were undertaken using DFT (6-31G\*) as implemented in the program SPARTAN '10 (Wavefunction, Inc., Irvine, CA) and as described in B. Stewart, A. Harriman and L. J. Higham, *Organometallics*, 2011, **30**, 5338-5343. For the radical cation of **3**, three local minima were refined, and the results depended on the orientation of the OH and PH<sub>2</sub> given as starting structures. These structures are depicted below. The two lowest energy isomers differ by only 0.5kcal/mol.

### Scheme S1.



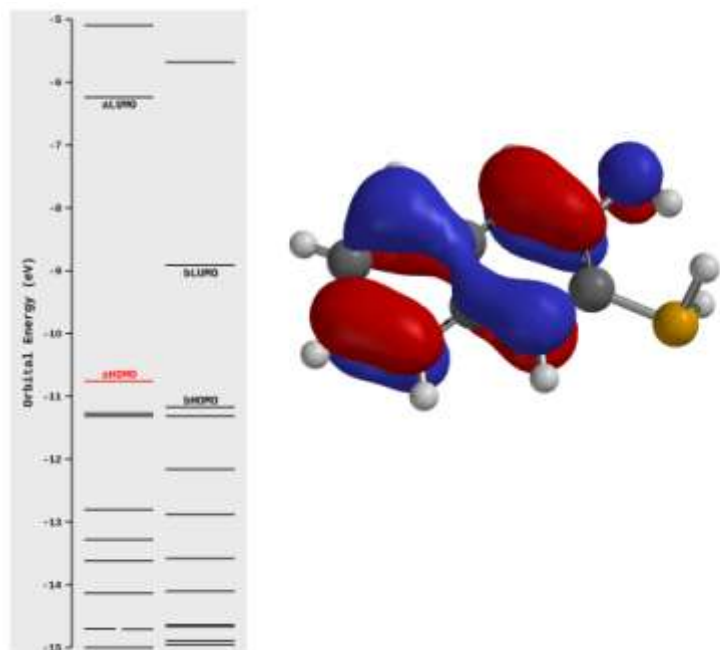


**Figure S23.** Second lowest energy isomer for radical cation of **3**.

For the neutral **3**, two local minima were refined, and the results depended on the orientation of the OH and PH<sub>2</sub> given as starting structures. These structures are depicted below. The two isomers differed by just 0.2 kcal/mol.

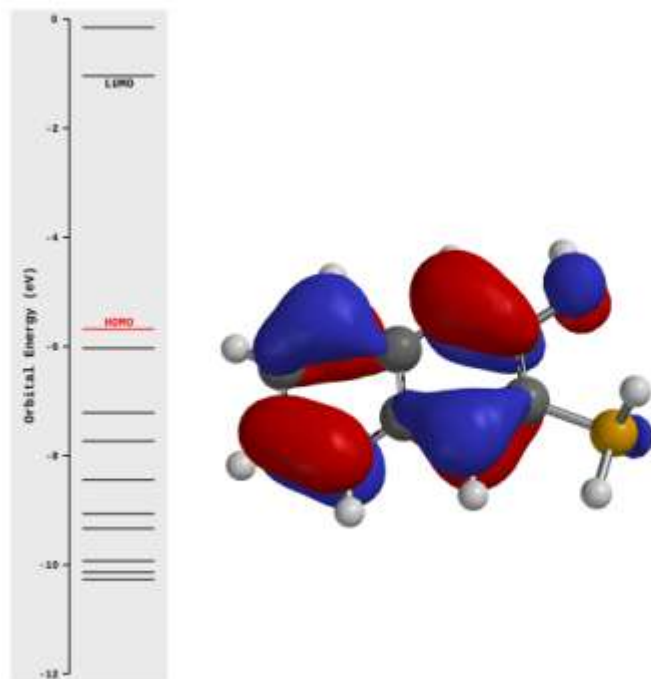


**Figure S24.** Lowest energy isomer for **3**.

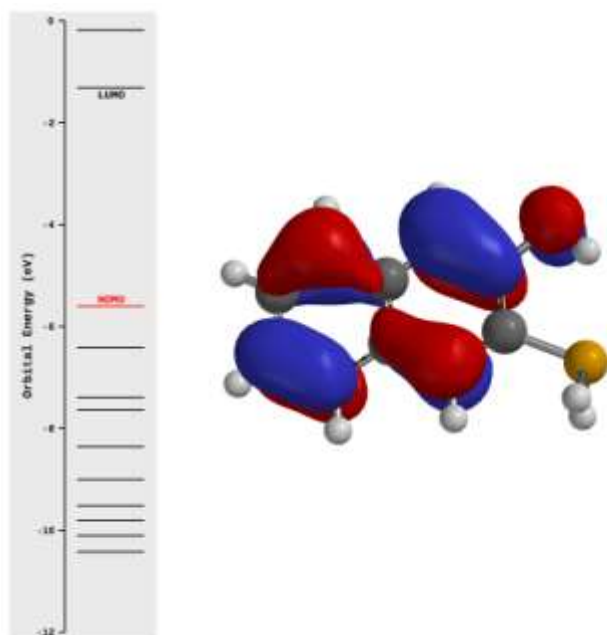


**Figure S25.** Next lowest energy isomer for **3**.